UJEAS

UNIZIK JOURNAL OF ENGINEERING AND APPLIED SCIENCES

UNIZIK Journal of Engineering and Applied Sciences 3(4), September (2024), 1220 - 1233
Journal homepage: https://journals.unizik.edu.ng/index.php/ujeas
PRINT ISSN: 2992-4383 || ONLINE ISSN: 2992-4391

Development and performance evaluation of balling disc machine for laboratory applications

Obuora A. Okoye[1*], Ifeanyi J. Okafor[2], Ugochukwu P. Ochieze[3], Sam N. Omenyi[4]
[1,2]Department of Mechanical Engineering, Michael Okpara University of Agriculture, Umudike
[2]Department of Project Management, University of West Scotland, Paisley, Scotland
[3]Department of Materials & Metallurgical Engineering, Federal University of Technology, Owerri
[1,4]Department of Mechanical Engineering, Nnamdi Azikiwe University, Awka
[*]Corresponding Author's E-mail: okoye.obuora@mouau.edu.ng

Abstract
This paper presents the design, development and performance evaluation of a balling disc machine which was resized for laboratory applications. The unavailability of a balling disc machine in the laboratory, to agglomerate powders for research purposes, prompted this endeavor. Balling disc machines are used to agglomerate powder materials into spherical forms by using an electric motor, shaft, pulleys and driving belts to apply rotational motion to the balling chamber. The balling chamber has three hanging rods that is massing the powders particles together against the balling cylinder wall into larger agglomerates. The objective is to design a balling machine with balling speed not exceeding 30 rpm, construct it and evaluate its performance. The design applied fundamental engineering and mathematical expressions to determine the machine components. The designed machine components values were used to construct it by welding them together and painting. The design presented the shaft length as 157 mm, shaft power as 0.446 KW, shaft diameter as 40 mm, balling cylinder volume as 7.44×10^5 mm^3, hanging rods diameter and length as 4.2 mm and 37.5 mm respectively. Four different powders and a binder were used to test the balling machine agglomeration performance. Throughput, agglomerate efficiency and machine efficiency were the parameters evaluated to exhibit the machine's performance. Powder C reported the highest throughput value of 0.54 g/sec and Power D had the lowest throughput value of 0.24 g/sec. Powder B and C reported the highest agglomeration efficiency values of 92.0% and 92.3% respectively while Powder A and D reported agglomeration efficiency values of 91.5% and 91.2% respectively. Powder B reported the highest machine efficiency value of 87% and Powder A reported the lowest value of 84.3%. The evaluated parameters revealed the effectiveness of the balling disc machine and fulfilled its objective in the production of powder agglomerates. The powder agglomerates produced were found to be within desired requirements and they are suitable for further experimental analysis and applications. The balling disc machine fulfilled its objective and functioned excellently in the laboratory.

Keywords: Powder, Binder, Machine efficiency, Throughput, Agglomeration efficiency, Hanging rods

1. Introduction

Conventionally, for convenience during transportation, handling, processing, and for product formulations, materials in powder form are best transformed into pellets, granules or agglomerates. Balling disc machine can be used industrially in so many manufacturing and production industries, such as in agriculture, it is used in fertilizer and animal feed agglomeration (Ezewu 2021). In the mining industry, it is used to agglomerate powdery ores (Focus 2022) prior to leaching (CVIC, 2022; de Moraes et al., 2018; Udo et al., 2018a; Udo et al., 2018b), and in food industries, it is used in the production of beverages, chocolates, sweets, etc (Dhanalakshmi, Ghosal, and Bhattacharya 2011). The pelletization of biomass from different raw material sources for fuel (Milan, M., and Velimir. 2011; Shardul et al. 2018; Tondare et al. 2018) and also used in the pharmaceutical industry (Deb and Ahmed 2017; Dumpala, Patil, and Universiy 2020; Ikebudu et al. 2015; Jawahar and Patel 2012; Pathade, G., and B 2014). The uniqueness of the balling disc amongst other powder agglomeration processes and equipment lies in the high balling rate and peculiar spherical form of the end product formulation (Ikebudu, 2012).

Most industrial balling disc machines are built with an inherent circular arc structure such as the disc fertilizer granulator. The granulation plate includes three feed intake holes, which makes it ideal for intermittent production and lowers work intensity and increasing labor efficiency. The speed reducer and motor use a flexible belt transmission, which allows the equipment to start smoothly, reduce impact force, and extend its service life. Radiant steel plates are used to reinforce the plates, which are sturdy and never distort. The machine's anabatic, thickened, and sturdy base construction eliminates the need for anchor bolts, allowing for stable operation. The granulator's primary gear uses high frequency quenching, which doubles its service life. The granulation pan is made of high-strength fiberglass, making the machine extremely durable. The machine offers uniform granulation, a high granulation rate, reliable operation, sturdy equipment, and a long service life, making it an excellent choice for users.

There has been significant research and development focused on optimizing balling disc machines for industrial-scale production, much of the literature centres on large-scale equipment designed for high-volume output (Blum & Schräpler, 2004; Okechukwu, 2012). Industrial machines are typically large and complex, designed to meet the demands of high-capacity processing plants. They often incorporate advanced features such as multiple feed intake holes, high-frequency quenching for extended gear life, and flexible belt transmissions that reduce impact forces during operation (Henan, 2022). These machines are designed to operate continuously under heavy loads, making them ideal for large-scale applications but impractical for smaller, more controlled environments such as research laboratories.

However, there are a number of difficulties in modifying these massive industrial machinery for use in laboratory settings. Smaller, more adaptable equipment that can handle smaller amounts of material and run efficiently on less electricity is frequently needed in laboratories. Furthermore, industrial balling disc machines are too large and expensive for the controlled, limited space settings of research and university labs. There is a glaring lack of balling disc machines made especially for laboratory usage, where accuracy, adaptability, and affordability are crucial, despite the substantial developments in industry. The presented design provide significant advantages in terms of accessibility for educational and research institutions and lower cost against the industrial ones. The use of locally sourced materials and simplified mechanical components makes the machine easier to maintain and operate compared to more complex industrial systems.

Currently, lots of powder agglomeration processes have been put forward in various manufacturing and production industries which have been significantly effective industrially. However, the challenge of handling and processing powder materials in the laboratory gave rise to this project. The industrial balling disc machines are physically in large sizes and this creates hindrances in the laboratory (Henan 2022). During product formulations using powdered raw materials, the product stability, dispersability, flowability, etc. are paramount. The powders products have been seen as smooth agglomerates in spherical form when applying the balling disc machine. Most powder agglomeration processes are mechanized either in the form of pelletizer, granulator or balling which transforms the powdered materials to either pellets, granules or balls respectively (Vo et al. 2018). The unavailability and inaccessibility of a balling disc machine in a laboratory for effective handling of novel powders led to conceiving the idea of fabricating one. This study presents the design and construction of a balling disc machine with special emphasis for agglomerating powder into uniform and spherical shapes. An evaluation of the machine's performance was also reported. Agglomerates produced using the balling disc machine by the introduction of pre-mixed binding liquid and powder particles, are bonded together by superficial interface which maximizes particle to particle surfaces adhesion and cohesive bonds between powder particles and binding fluids. Fulfilling the need of a laboratory size balling disc machine for research purposes contributes as a unique attempt to be resourceful in challenging circumstances.

2.0 Material and methods

2.1 Machine description

Figure 1(a) is computer software (SolidWorks) generated design of the balling disc machine. The picture shows the various parts and components of the machine such as electric motor, pulleys, driving belt, balling cylinder, shaft, ball bearing and machine frame. The machine starts smoothly due to the speed reducer which slows down the impact and improves equipment service life. The process of operation involves - manually putting the powder into the cylindrical disc, addition of appropriate binding fluid, properly covering the lid, and switching on the machine through the electric motor switch. During operation, torque is generated on the shaft to the cylinder disc via the transmission system, which consists of two pulleys, a belt, and the cylindrical disc's shaft. Hanging rods shown in Figure 1b are attached inside the cylindrical disc in a regular triangular form (60^{o} spacing) which aids the balling of the agglomerates to maintain an average diameter of 20 mm, as the cylindrical disc rotates. The rods' rotational motion puts a force on the powder and binding fluid, pressing them against the disc's walls.

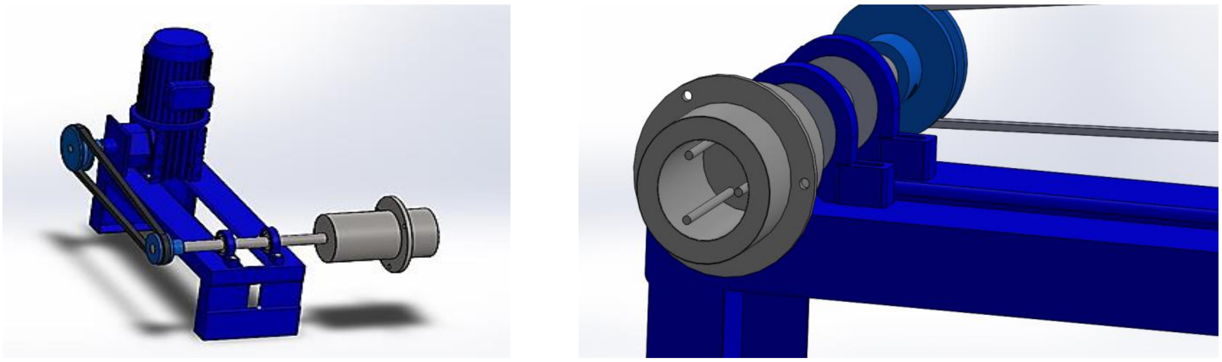

(a) **(b)**

Figure 1: (a) Isometric view of the balling disc machine (b) Balling disc interior showing the hanging rods, separated at 60^o equidistant to one another.

2.2. Design requirements

The general requirements for this design are:

- Production of continuous rotational motion.
- Introduction of the powder – binding fluid mixture.
- Production of spherical agglomerates uniformly shaped by the machine rotation.
- Steady discharge of the spherical agglomerates with minimal distortion.

2.3. Material selection

Considerations in material selections include: good mechanical properties of available materials sourced locally, noise reduction (since it will be used in the laboratory), economical cost of machine production, simple maintainability, and machine aesthetic. The cylinder disc and shaft composed of an austenitic stainless steel material, the base composed of mild steel C1345, and gloss blue paint, used for painting the machine base to prevent wear, corrosion, and add aesthetics. The forming and joining processes were mostly by turning and electric arc welding. The shaft bearing and electric motor were fastened with bolts and nuts.

2.4. Machine components description and design

2.4.1. Electric motor

The balling disc machine's main power source is the electric motor. It provides the balling disc the rotational energy. Low speed guarantees that powder agglomerates are uniformly and spherically formed. The design for motor output power enables appropriate selection of an electric motor. Omenyi et al., (1983), Blum & Schräpler, (2004); Henan, (2022) affirmed that agglomerate formation in a balling disc under gravitational attraction forms best at low velocity rotation or moderate balling speeds. Rumpf, (1962) formed agglomerates using an inclined granulating disc rotating at 12 rpm. At 23 rpm, agglomerates were satisfactorily obtained by Newitt & Conway-Jones, (1958). In order to obtain the required low speed for optimum agglomerates formation, the balling cylinder speed was not to exceed 30 rpm and a 0.5hp electric gear motor with speed of 950rpm was selected for the design.

2.4.2 Shaft

The shaft transfers the rotational force to the disc. The shaft is composed of a robust material to withstand mechanical pressures during operation, and it is supported by bearings to ensure smooth rotation. Its diameter and length are designed to maintain stability while handling the torque produced by the motor. The maximum load capacity of the electric motor given by the shaft power is computed from the expression in Equation (1);

Shaft power = input power x service factor (1)

where input power = **0.5 hp** = **0.3728 KW**, service factor = **1.25** as recommended by Learning, (2016).

Shaft power = 0.3728 x 1.25 = ***0.466 KW.***

2.4.3 Pulley and belt drive system

The transmission of rotational energy from the electric gear motor to the balling disc is facilitated by the pulley and belt system. A flexible belt connects the two pulleys, providing smooth operation. The gear motor carrying the big pulley is mounted on the shaft of the electric motor. The big pulley transmits rotational motion via a belt drive to the small pulley incorporated on the shaft of the balling cylinder while balling cylinder shaft is held in position by two radial bearings fastened to the machine frame. The pulleys material are made from aluminum alloy and the weight is negligible on the shaft.

2.4.4 Pulley diameter

The Martin catalogue V-pulley (Martin Sprocket & Gear 2011) recommended 560mm (Driver pulley, D_1) and 280mm (Driven pulley, D_c) standard pulleys corresponding to the speed ratio or velocity ratio between the electric motor and gear motor as **190:3**. The driver pulley speed (N_S) was determined by applying Equation (2). The balling cylinder speed (N_c) was computed from Equation (3) whose results are **15 rpm** and **30 rpm** respectively.

$$VR = \frac{N_m}{N_S} \tag{2}$$

$$VR = \frac{950}{15} = \mathbf{190:3}$$

$$N_S D_1 = N_c D_c \tag{3}$$

2.4.5 Theoretical centre distance

Belt selection was computed from the pulley pitch diameters and the center distance of the two pulleys. The center diameter computed as the distance between the mid-point of big pulley and that of the small pulley to set limits of the belt length . Khurmi & Gupta, (2008b) expression for the center distance given in Equation 4 was employed

$$C = \frac{1.5D_c}{(VR)^{0.3}}\ ,\ mm \tag{4}$$

The center distance was calculated to be **341.15 mm**.

The theoretical belt length was then computed to be **2058.553 mm** with the pitch diameters of the two pulleys, D_1 = 560mm, D_2 = 280mm and center distance = 341.13mm, using Equation 5.

$$L = 2C + 1.57(D_c + D_1) + \frac{(D_c - D_1)^2}{4C},\ mm \tag{5}$$

2.4.6 Belt tension on driver pulley

The belt tension (T_1) acts on the tight side of the belt on the driver pulley and the tension (T_2) acts on the slack side of the belt on the driver pulley. The values of T_1 and T_2 are computed using Equations (6 – 10);

$$\frac{T_1}{T_2} = e^{\mu_e \theta} \tag{6}$$

where $\mu_e = \frac{\mu}{\sin\frac{\beta}{2}}$; $\theta = \pi + 2\sin^{-1}\frac{D_C - D_1}{2C}$

$$Design\ Power = \frac{(T_1 - T_2)V}{1000}\ ,KW \tag{7}$$

where $V\ (Velocity\ of\ belt) = \frac{\pi\ x\ D_1 \times N_S}{60 \times 1000}\ ,m/s$

So, $T_1 - T_2 = \frac{0.466 \times 1000}{0.44} = \mathbf{1059.5\ N}$ (8)

Also, $\frac{T_1}{T_2} = e^{0.983 \times 3.99} = \mathbf{50.5099}$ (9)

$$T_2 = \frac{1059.6}{49.5099} = \mathbf{21.402\ N}$$

$$T_1 = 134.16 \times T_2 = \mathbf{1081.01\ N} \tag{10}$$

T_1 and T_2 are computed with values for belt friction on pulley, μ, and pulley groove angle, β as **0.32** and **38°** respectively. Torque acting on the driver pulley, T_A, was computed as ***296.72 Nm*** and power transmitted, P_A, to the driven pulley from the driver pulley to be ***466 W*** using Equations (11) and (12) respectively.

$$Torque\ at\ driver\ pulley, T_A = (T_1 - T_2)\frac{D_1}{2};\ Nm \tag{11}$$

$$Power\ transmitted,\ P_A = \frac{T_A\ x\ 2\ x \pi\ x\ N_S}{60};\ W \tag{12}$$

The belt tension (T_3) acts on the tight side of the belt on the driven pulley and the tension (T_4) acts on the slack side of the belt on the driven pulley. The values of T_3 and T_4 are computed using Equations (6 – 9) & (13);

$$Torque\ at\ driven\ pulley, T_B = (T_3 - T_4)\frac{D_C}{2};\ Nm \quad (13)$$

Belt tensions on the driven pulley computed as $(\boldsymbol{T_3})\mathbf{1081.01}\ \boldsymbol{N}$ and $(\boldsymbol{T_4})\ \mathbf{21.402}\ \boldsymbol{N}$ which are the same as the belt tensions on the driver pulley.

2.4.7 Balling cylinder

The balling cylinder, also referred to as balling disc, is the focus of this machine and the section where powder agglomeration takes place. Stainless steel was used to enhance durability and resistance to wear and corrosion inside the revolving cylindrical chamber. Powder agglomeration occurs as the balling cylinder rotates and through physical bonding mechanism, the powder and binding fluid bind together. This physical bonding mechanism is achieved by the formation of intermolecular bonds between the powder particles and binding fluid (Szulc et al. 2024). Hanging rods are found inside the balling chamber because they aid powder agglomeration to achieve the desired uniform and spherical shapes. Stainless steel with density, ρ_S, of **8x10^{-6} kg/mm^3** was selected as the material for the balling cylinder. The need to eliminate or reduce friction as foreseen in material loss during operation necessitated the selection. Volume of the cylinder was computed using Equation (14)

$$Volume\ of\ balling\ cylinder, V_C = \pi\ x\ r^2\ x\ h,\ mm^3 \quad (14)$$

where the dimensions of the balling cylinder are *95 mm* x *105 mm* being the diameter and length of the balling cylinder respectively. The balling cylinder volume was calculated to be $\mathbf{744262.935}\ \boldsymbol{mm^3}$ and mass of balling cylinder computed to be $\mathbf{5.95}\ \boldsymbol{kg}$ using Equation (15).

$$Mass\ of\ balling\ cylinder, M_C = density \times volume,\ kg \quad (15)$$

2.4.8 Design of hanging rods

Hanging rods are found inside the balling chamber and aid in making the powder agglomerates take a uniform and spherical shape. The length of the hanging rods is chosen to ensure optimal material agitation without interfering with the bottom of the balling cylinder. The length, L, of the hanging rods was based on the radius, r, of the balling cylinder and a clearance, *h*, to prevent drag. (Hibbeler 2019) and computed from Equation (16) as

$$L = r - h;\ mm \quad (16)$$

Hanging rods length was computed to be $3\mathbf{7.5}\ \boldsymbol{mm}$**.**

2.4.8.1 Diameter of the hanging rods

The hanging rods are stainless steel rods that are designed for strength, durability and resistance to corrosion. The design was to prevent material clogging and excess drag (Budynas and Nisbett 2015). Stainless steel of yield strength, σ_y, of $2\mathbf{50}\ \boldsymbol{MPa}$ was used to compute the hanging rods diameter by applying Equation (17) because they must withstand the bending forces encountered while carrying out its function (Beer et al. 2016). The bending moment can be computed as

$$\sigma_b = \frac{M_H}{I} \quad (17)$$

$$I = \frac{\pi d^4}{64} \quad (18)$$

The bending moment calculation was applied in the form of a standard cantilever beam model and computed as $M_H = F_{total} * L$ (19)

$$F_{total} = \left[\rho\left(\frac{\pi d^2}{4} * L\right) + \frac{6}{1000}\right] * g \quad (20)$$

where $g = 9.81\ m/s^2$ and the hanging rod diameter is obtained as $4.2\ mm$ from Equation (21). The hanging rods are three in number and are welded to the base of the balling cylinder.

2.4.9 Torque on balling cylinder shaft

The torque transmitted to the balling shaft was computed to be **148.33 Nm** using Equation (21). The torque is the maximum stress that the balling cylinder shaft has to withstand with the assistance of the radial bearings and frame.

$$T_B = \frac{P_A \times 60}{2 \times \pi \times N_C};\ Nm \quad (21)$$

2.4.10 Shaft diameter

Sharma & Aggarwal, (2013) stipulated that commercial steel shaft without specifying its physical properties has a maximum value for design stress, $f_s = 55\ MN/m^2$. The shaft is assumed to be cylindrical and its weight evenly distributed across its length. The shaft diameter is determined from the maximum normal stress on the shaft which consists the shaft's bending moment analysis and balancing of all forces acting on the shaft of length, l_s, $157\ mm$. The forces acting on the shaft were resolved vertically and horizontally.

Resolving the forces vertically; $51.3R_B = -(59.5 \times 56.24)$ (22)

$R_B = -65.24\, N.$

Equating forces acting upwards to forces acting downward in order to attain for force equilibrium in the shaft

$59.5 = -65.24 + R_C$ (23)

$R_C = 124.74\, N$

Computing vertical bending moment;

At $D, BM_D = 0\, N - mm$ (24)

At $C, BM_C = (59.5 \times 56.25) = 3346.9\, N - mm$ (25)

At $B, BM_B = (59.5 \times 107.55) - (124.74\, x\, 51.3) = 0\, N - mm$ (26)

At $A, BM_A = (59.5 \times 157) - (124.74 \times 100.75) + (65.24 \times 49.45) - (15.45 \times 49.45) = 0\, N$ (27)

Resolving the forces horizontally; $-1102.412 = 51.3R_C$ (28)

$R_C = -1062.656\, N$

Equating forces acting upwards to forces acting downward in order to attain for force equilibrium in the shaft

$1102.412 = -1062.656 + R_B$ (29)

$R_B = 2165.068\, N$

Computing horizontal bending moment; At $A, BM_A = 0\, N - mm$ (30)

At $B, BM_B = (1102.412 \times 49.45) = 54514.27\, N - mm$ (31)

At $C, BM_C = (1102.412 \times 100.75) - (2165.068 \times 51.3) = 0\, N - mm$ (32)

At $D, BM_D = (1102.412 \times 157) - (2165.068 \times 100.75) + (1062.656 \times 78.5) = 0\, N - mm$ (33)

The resultant bending moment along the constrained and unconstrained points on the shaft becomes

At $E, = 0\, N - mm$ (34)

At $D, = 0\, N - mm$ (35)

At $C = 3346.9\, N - mm$ (36)

At $B = 54514.27\, N - mm$ (37)

At $A = 0\, N - mm$ (38)

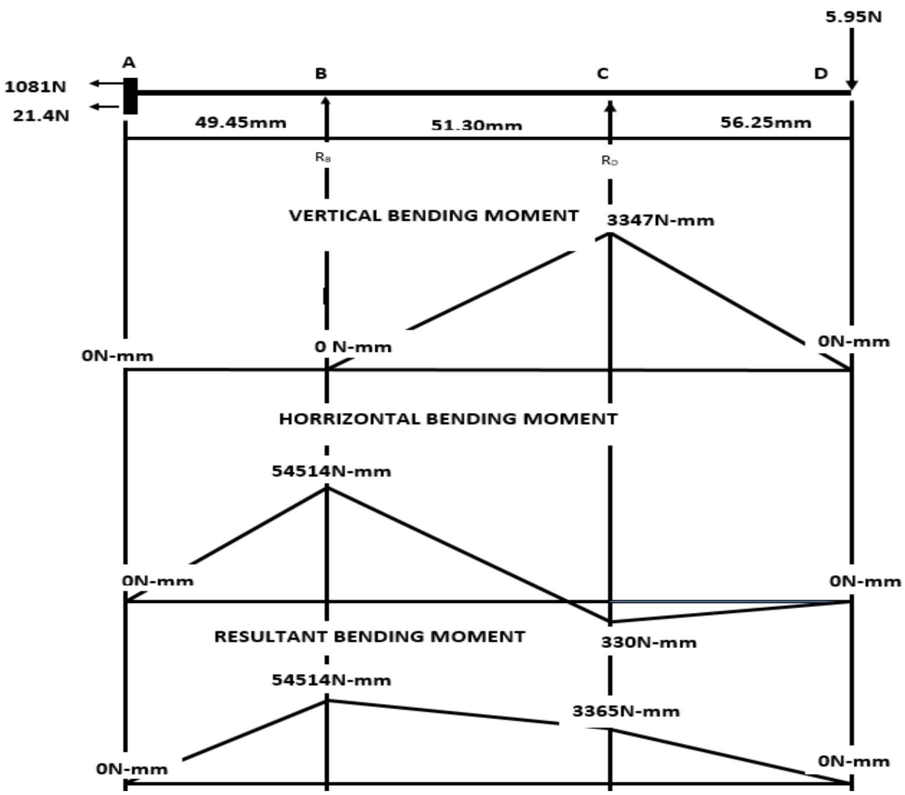

Figure 2: Bending moment diagram of balling cylinder shaft

The shaft diameter is calculated from Equation (39), whereby K_b and K_s (constant factors for steadily applied loads and minor shock) with values 1.5 and 1.0 respectively.

$$Shaft\ diameter, d\ =\ \sqrt[3]{\frac{16}{\pi f_s} * \sqrt{(K_b * M_b)^2 +\ (K_S * T_B)^2}}\ , mm \qquad (39)$$

The total maximum bending moment, M_b, is computed using Equation (40) whereby the horizontal and vertical resultant moment are M_h and M_v respectively. The total bending moment calculated equals $\mathbf{54,616.65\ Nmm}$.

$$M_b\ =\ \sqrt{\left({M_h}^2 +\ {M_v}^2\right)}\ Nm \qquad (40)$$

A consideration is given to the induced stress concentrations in shaft occasioned by the cutting of keyway on the shaft. This affects the design stress to the tune of Equation (41) and the appropriate design stress equals **41.25 MN/m^2**.

$$Design\ stress, f_s\ =\ (0.75)\ \times\ design\ stress\ of\ shafts\ without\ keyway,\ N/m^2 \qquad (41)$$

Thereby substituting the appropriate values as determined in Equations (40 and 41) into Equation (39), the shaft diameter, d = **0.03946m = 39.5 mm.** The shaft diameter is selected from the available standard shaft sizes to be **40 mm**.

Maximum shear stress on the shaft for combined load due to torsion and bending is computed using Equation (42) which was determined as **12578561.32 N/m^2**. But the pure torsion load, f_s and pure bending load, f_t were also computed using Equations (38) and (39) equal to **11803726.35 N0/m^2** and **8693042.99 N/m^2** respectively.

$$Maximum\ shear\ stress, (f_s)_{max}\ =\ \frac{1}{2}\sqrt{{f_t}^2 + 4{f_s}^2}\ , N/m^2 \qquad (42)$$

Pure torsion load, $f_s\ =\ \frac{16\ x\ T_B}{\pi d^3}\ ,\ N/m^2$ (43)

Pure bending load, $f_t\ =\ \frac{32\ x\ M_b}{\pi d^3}\ ,\ N/m^2$ (44)

The weight of the shaft is computed using Equations (14) and (15) to be **6.31 kg**.

2.4.10 Selection of shaft bearings

Bearings enable smooth rotation and support the shaft. They are placed in key locations where the shaft rests on the machine frame. These bearings are designed to withstand loads applied to the shaft both axially and radially while operating. This ensures the shaft moves smoothly, frictionless and guards against misalignment. The balling machine has two radial ball bearings which were selected to form the shaft support, guide and confine the shaft motion. They withstand radial and axial loads exerted on the shaft and also transmit these loads to the machine frame. With the determined shaft diameter and reactions on the shaft supports, a bearing expected life span of 10 years, 300 days for 4 operational hours per day was having 12,000 hours of operation. Bearing life was computed to be 21.6x10^6 revolutions. These values were computed using Equations (45 and 46) and dynamic equivalent radial load (W) using Equation (47).

$$L_H = 10 \times 300 \times 4 = 12{,}000\ hrs \qquad (45)$$

$$Lr = 60\ x\ N\ \times\ L_H = 60\ x\ 30\ \times\ 12000 = 21.6\ \times\ 10^6\ rev. \qquad (46)$$

$$W = X.V.W_R + Y.W_A,\ N \qquad (47)$$

Since there are no thrust loads present, the radial load was determined for the left and right bearings as **2166.05N** and **1069.96N**. The dynamic load rating for the left and right bearings were computed using Equation (48) and determined as $\mathbf{5.97\ KN}$for the left bearing and $\mathbf{2.95\ KN}$ for the right bearing.

$$Cr = W\left(\frac{L}{10^6}\right)^{0.33}\ ,\ KN \qquad (48)$$

By applying the dynamic load for both the left and right bearings and shaft diameter of 40mm, a radial ball bearing designation of ***W61908*** is selected for the left bearing and ***W61808*** is selected for the right bearing (SKF 2015).

2.4.11 Design of the frame

The machine frame serves as the structural foundation of the balling disc machine. The machine base was designed to withstand the torque generated by the electric motor, shaft and also support the weights of the electric motor, shaft and balling cylinder. The frame was designed using mild steel (C1345) angel iron of tensile strength of **290 N/mm^2** (Khurmi and J. K. Gupta 2008).

2.5. Machine construction

The machine was fabricated based on the design specification. The construction was carried out with locally sourced materials to reduce the cost of production. Machine design procedure shown in Figure 3 was observed in fabricating each component.

Table 1: Machine parameters and specifications

Design Parameter	Specification
Power of the electric motor	0.5hp
Diameter of cylinder shaft	40mm
Dynamic load on LHS bearing	5.97kN
Dynamic load on RHS bearing	2.95kN
Volume of balling disc cylinder	744262.935mm^3

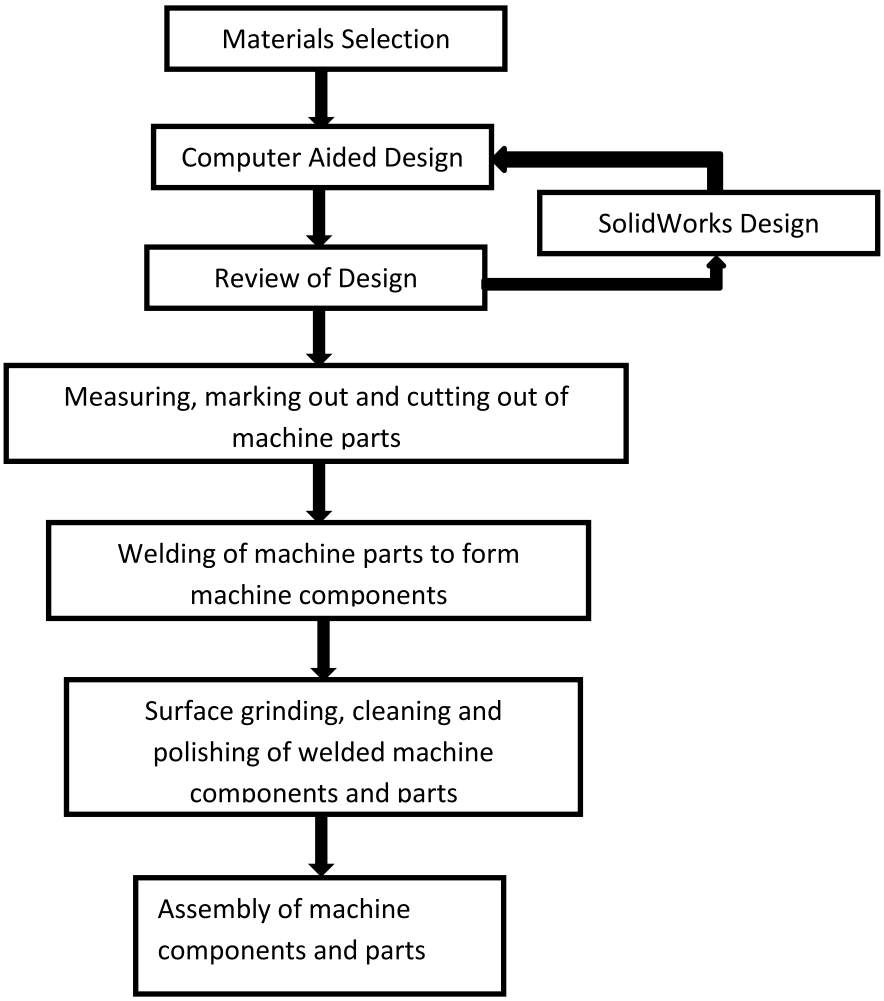

Figure 3: Chart of the design methodology, procedure and construction of balling disc machine.

Figure 4: Picture of the balling disc machine

3.0 Results and Discussions

3.1 Performance evaluation

Performance evaluation carried out on the balling disc machine were agglomeration efficiency, throughput and machine efficiency.

3.1.1 Agglomeration efficiency

The agglomeration efficiency of the machine was computed using Equation (49) and it's the ratio of the mass of the pellets/agglomerates produced W_p to the mass of the recovered output, W_o. The agglomerates where manually separated from the recovered output after which was weighed to determine the mass.

$$Aglomeration\ Efficiency\ = \frac{W_p}{W_o} \times \frac{100}{1},\ \% \quad (49)$$

3.1.2 Throughput

The throughput measures the rate at which the agglomerates are formed inside the balling cylinder. This was computed using Equation (50) and also measures the quantity of output produced by the machine per unit time.

$$Throughput, T_p\ = \frac{W_0}{t},\ g/sec \quad (50)$$

3.1.3 Machine efficiency

The machine efficiency is the ratio of the mass of the all recovered output W_o to the mass of the input feed W_i. The recovered outputs is mass summation of both agglomerated and non-agglomerated residual powder and binder mix that stuck on the walls of the cylinder, which was obtained using Equation (51).

$$Machine\ efficiency, \eta\ = \frac{W_o}{W_i} \times 100,\ \% \quad (51)$$

At the conclusion of the design and construction of the balling disc machine, determination of the performance index was done by evaluating Equations (49, 50 and 51). Four different powders and a binder were used to ascertain the agglomeration efficiency, throughput and machine efficiency. The powders were premixed as in Omenyi & Capes, (1982) and introduced into the balling cylinder. The electric motor was turned on and rotational energy was transmitted through the belt drive and balling cylinder shaft to the balling disc. Agglomeration time, mass of agglomerates and agglomerate diameter are some of the data recorded using a stop watch, weighing scale and Vernier caliper respectively. The agglomerate powders formed are removed from the balling cylinder using a stainless spatula for appropriate measurements. The mass of powder and binder that were premixed, balling time and mass of agglomerate produced are recorded in Table 2.

Table 2: Agglomeration properties of different powder material

Powders	Mass of Powder (g)	Mass of Binder (g)	Balling time (s)				Mass of Agglomerates (g)
			T_1	T_2	T_3	Average Time	
A	6	2.00	14.26	15.26	12.20	13.39	5.90
B	6	3.75	16.82	17.34	16.32	16.83	7.61
C	6	2.70	21.23	23.45	23.43	22.70	6.52
D	6	3.85	31.33	32.43	30.56	31.44	7.65

Performance evaluation of the balling disc machine using the data presented in Table 2 are presented in Table 3 and plots were generated to discuss these results.

Table 3: Performance evaluation of balling machine

Powders	Throughput (g/sec)	Agglomeration Efficiency (%)	Machine Efficiency (%)
Powder A	0.44	91.5	84.3
Powder B	0.45	92.0	87.0
Powder C	0.54	92.3	84.7
Powder D	0.24	91.2	86.4

3.2 Throughput

The machine, as depicted in Figure 4, gave high throughput for the four sample powders used in evaluating it. Though sample powder C had the highest throughput value, sample powder D gave the lowest while samples powder A & B had almost the same throughput value. The essence of determining the machine throughput is to establish the amount of agglomeration the machine can achieve within a stipulated timeframe. Differences in the throughput values for the sample powders can be ascribed to the physical and chemical properties of the various powders and binder. These physical and chemical properties identifies each powder sample and the interaction with the binder to aid in the forming of interstitial bonds by exchanging surface energies created by the frictional rotation of the balling cylinder. The binder action on the powder samples renders the powder sample particles to have a sticky surface (Barkouti et al. 2013; Dhanalakshmi et al. 2011) and this aids agglomeration of powder particles. The difference amongst the sample powders physical and chemical properties and its interaction with the binder accounts for the throughput for each powder sample.

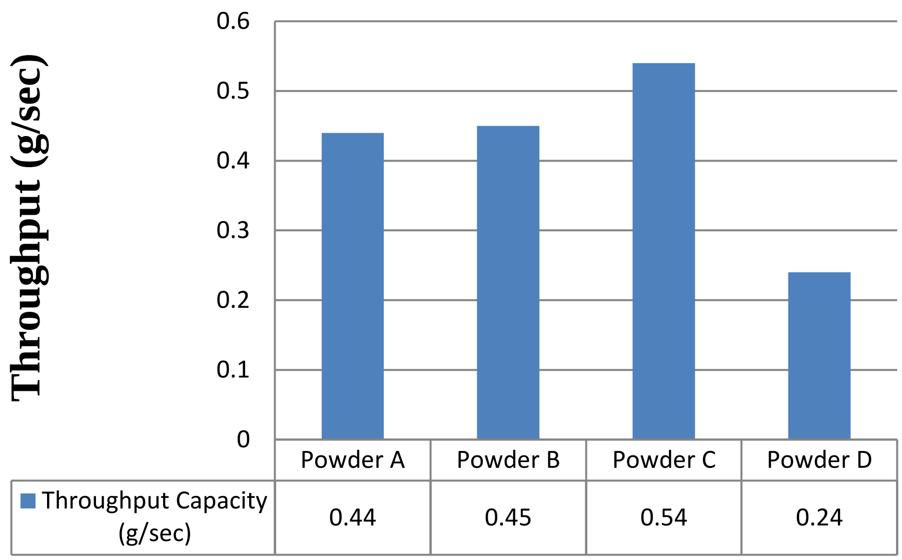

Figure 5: Plot of the Throughput Capacity against Powders

3.3 Agglomeration efficiency

The agglomeration efficiency of the machine for the four sample powders is shown in Figure 5. Powder sample C turned out more agglomerated powders than the others while powder D was the least. Unlike the throughput capacity, powder samples A & B were within the highest and lowest agglomeration efficiencies with powder sample B higher than powder sample A. Agglomeration efficiency explains the powder sample that gave the highest output of agglomerated products in a selected powder sample. Powder sample D when mixed with the binder became loose fluffy aggregates which is a powder transformation process that can be explained in a phenomenon resulting from the surface tension of the binding liquid. The surface tension becomes a driving force which occurs by the reduction of the total surface free energy of the system that accompanies the decreased air-liquid interfacial area (Vo et al. 2018). Fröhlich et al., (2023) determined the agglomeration efficiency of agglomerates formed as drying droplets collide with dry particles. The agglomerate efficiency was defined as the number of successfully adhered primary particles per recirculation and Equation (49) represents this definition.

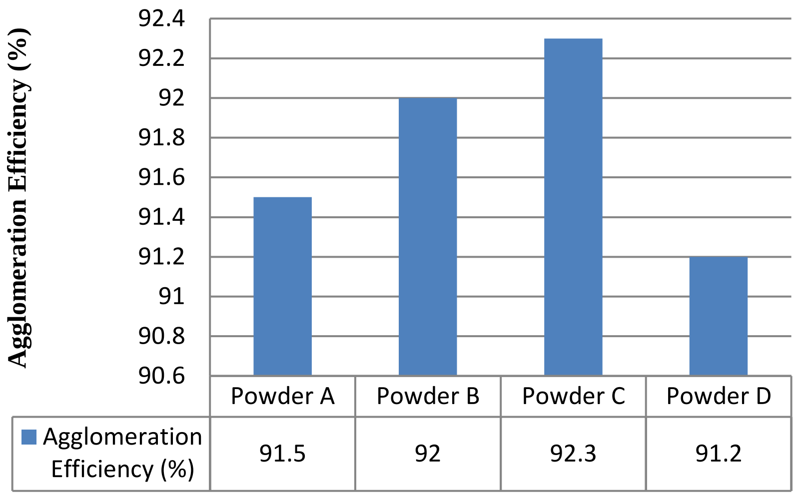

Figure 6: Plot of Agglomeration Efficiency against Powders

3.4 Machine efficiency

Machine efficiency is depicted by Figure 6 for the four powder samples. Using the balling machine to agglomerate different powder samples showed a different trend from agglomeration efficiency. Powder sample B had the highest machine efficiency followed by powder sample D, C and A in that order. It was interesting to note that though the physical and chemical properties of the powder sample and binding liquid are of utmost importance, the agglomeration time can be seen to become another input variable that can influence agglomeration in the balling disc machine. Time for agglomerating powder sample D is twice when compared to powder sample B. The balling machine gives higher machine efficiency within ranges of 15 to 17 minutes of rotational motion. This suggests that agglomeration of the powder samples were more effective within these time ranges while de-agglomeration may be occurring when the balling time is either less or more than this time range.

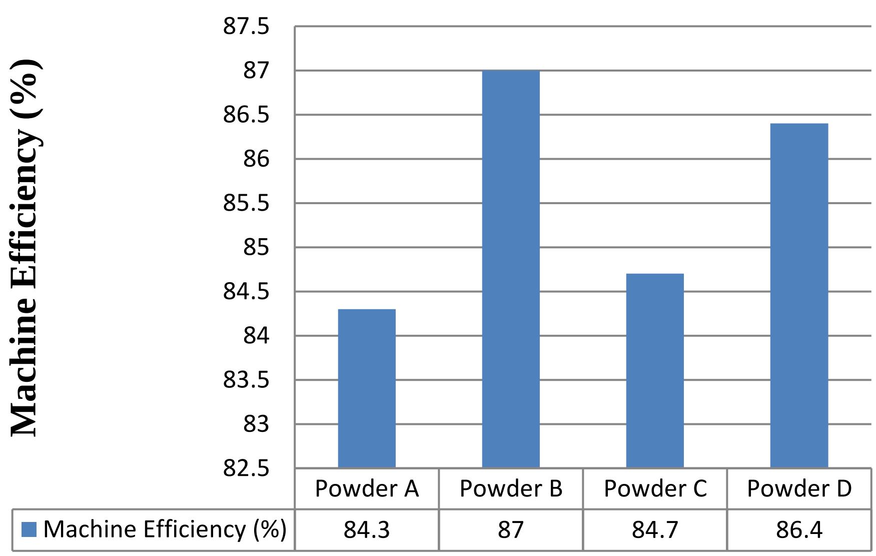

Figure 7: Plot of Machine Efficiency against Powders

4.0. Conclusion

The balling disc machine was adequately developed using Solid Works software, designed and constructed using locally sourced materials for mechanical engineering laboratory applications. The design was achieved by applying established mathematical and engineering formulae and procedures. The developed balling disc machine was found to be appropriate for the mechanical engineering laboratory and produced agglomerated powder samples as desired. The performance evaluated were agglomeration efficiency, throughput and machine efficiency. Powder C reported the highest throughput value of 0.54 g/sec and Power D had the lowest throughput value of 0.24 g/sec. Powder B and C reported the highest agglomeration efficiency values of 92.0% and 92.3% respectively while Powder A and D reported agglomeration efficiency values of 91.5% and 91.2% respectively. Powder B reported the highest machine efficiency value of 87% and Powder A reported the lowest value of 84.3%. Experiments conducted using four sample powders revealed the importance of the physical and chemical properties of the powder samples and binder for all performance parameters. It becomes evident that physical and chemical properties of the powder samples and binder played a crucial role in the effectiveness of the balling machine processes. This research revealed that, in order to agglomerate powder mixtures successfully, parameters such as mixture composition, particle size, percentage of added water and ambient conditions can be well coordinated and controlled to get agglomerates with optimal quality. Most importantly, the balling disc machine performance evaluation offers valuable perspectives and knowledge of the variations between different powders which makes it suitable for laboratory applications.

5.0 Recommendation

Adoption of this balling disc machine in mechanical engineering laboratories is highly recommended. It is working effectively and conveniently. The project is of benefit and as a teaching aid. More importantly, this machine is recommended to scholars for further research and improvement. Further research and improvement can focus on

1. Investigating on the balling characteristics properties of the powders and binders that aid fast agglomeration
2. Investigating how the balling machine parameters influence agglomeration of the powders
3. Investigating the powder-mixing kinetics of the machine.

.

Acknowledgements

Acknowledgements to my co-authors: Prof. S. N. Omenyi for the mentorship and supervision, Engr. I. J. Okafor for your CAD skills and Engr. U. P. Ochieze for your fabrication skills.

Nomenclature

C	Theoretical center distance, *m*
Cr	Dynamic load rating, *N*
d	Diameter of the shaft, *m*
d	*Diameter of hanging rod, m*
D_C	Cylinder shaft pulley diameter, *m*
D_1	Driver pulley diameter or speed reducer pulley diameter, *m*
f_S	Design stress, N/m^2
f_s	Pure torsion load on the shaft, N/m^2
f_t	Pure bending load on the shaft, N/m^2
$(f_s)_{max}$	Maximum shear stress on the shaft, *Nm*
F_{total}	Total force acting on the hanging rods, *N*
g	Acceleration due to gravity, m/s^2
h	Height of balling cylinder, *m*
I	Second moment of area for a cylindrical rod, m^4
K_b	Constant factors for steadily applied loads
K_S	Constant factor for minor shock
L	Theoretical belt length, *m*
l_s	Length of shaft, *m*
L	Length of hanging rods, *m*
L_H	Bearing expected life span in hours, *hrs*
Lr	Bearing expected life span in hours, *hrs*
M_b	Maximum bending moment on the shaft, *Nm*
M_C	Mass of balling cylinder, *kg*
M_h	Resultant maximum horizontal bending moment, *Nm*
M_H	Maximum bending moment of hanging rods, *Nm*
M_v	Resultant maximum vertical bending moment, *Nm*
N_C	Cylinder shaft speed, *rpm*
N_m	Electric motor speed, *rpm*

N_S	Driver pulley or speed reducer pulley, *rpm*
P_A	Power transmitted by the shaft, *W*
r	Radius of balling cylinder, *m*
R_B	Reaction at the left hand bearing, *N*
R_C	Reaction at the right hand bearing, *N*
T_A	Torque or Twisting moment at the driven pulley, *Nm*
T_B	Torque transmitted to the balling shaft, *Nm*
T_C	Centrifugal tension in belt, *N*
T_1	Tensions on tight side of the belt, *N*
T_2	Tensions on the slack side of the belt, *N*
V	Friction factor for multi-purpose bearing
V	Rotation factor of bearing
V_C	Volume of balling cylinder, m^3
V_{R1}	Speed ratio between electric motor and speed reducer
W	Dynamic equivalent radial load, *N*
W_A	Constant axial or thrust load, *N*
W_R	Combined radial load, *N*
X	Radial load factor
Y	Axial or thrust load
θ	Lap angle on the smaller pulley, *radians*
β	Groove angle of the pulley, *degree*
μ_e	Coefficient of friction of the belt and pulley
ρ_S	Density of stainless steel, kg/m^3
σ	Max allowable safe stress of belt, N/m^2
σ_b	Bending moment of hanging rods, Nm
σ_{ys}	Yield strength of stainless steel, N/m^2

References

Barkouti, Amal, Christelle Turchiuli, J. A. Carcel, and E. Dumoulin. 2013. "Milk Powder Agglomerate Growth and Properties in Fluidized Bed Agglomeration." (July). doi: 10.1007/s13594-013-0132-7.

Beer, Ferdinand P., Jr. E. Russell Johnston, John T. DeWolf, and David F. Mazurek. 2016. *Mechanics of Materials*. New York: McGraw-Hill Education.

Blum, Jürgen, and Rainer Schräpler. 2004. "Structure and Mechanical Properties of High-Porosity Macroscopic Agglomerates Formed by Random Ballistic Deposition." *Physical Review Letters* 93(11):1–4. doi: 10.1103/PhysRevLett.93.115503.

Budynas, Richard G., and J. Keith Nisbett. 2015. *Shigley's Mechanical Engineering Design*. 10th Editi. New York: McGraw-Hill Education.

CVIC. 2022. "Balling Solutions." Retrieved March 1, 2022 (https://www.cvic.ca/balling-solutions).

Deb, R., and A. B. Ahmed. 2017. "Pellets and Pelletization Techniques." *International Research Journal of Pharmac* 4(4):90–95.

Dhanalakshmi, K., S. Ghosal, and S. Bhattacharya. 2011. "Agglomeration of Food Powder and Applications." *Critical Reviews in Food Science and Nutrition* 51(5):432–41. doi: 10.1080/10408391003646270.

Dumpala, Rajesh, Chirag Patil, and Parul Universiy. 2020. "A Review on Pellets and Pelletization Techniques." (August).

Ezewu, K. 2021. "Design of an NPK Fertilizer Pelletizer." (November). doi: 10.4314/njt.v40i5.9.

Focus, Technology Co. Ltd. 2022. "Balling Disc / Disc Pelletizer." Retrieved March 1, 2022 (https://jiangsuhongda.en.made-in-china.com/product/RCixvKyuSjVS/China-Balling-Disc-Disc-Pelletizer.html).

Fröhlich, J. A., N. A. Ruprecht, and R. Kohlus. 2023. "Nozzle Zone Agglomeration in Spray Dryers: Determination of the Agglomeration Efficiency in the Fines Return by Means of Agglomerate Properties and Residence Time Distribution." *Drying Technology* 41(12):1907–1923. doi: https://doi.org/10.1080/07373937.2023.2203224.

Henan, Zhengzhou Mining Machinery Co. Ltd. 2022. "Disc Granulator." Retrieved March 1, 2022 (https://www.zkcomp.com/product/disc-granulator.html).

Hibbeler, Russell C. 2019. *Engineering Mechanics; Statics and Dynamics*. 14th editi. Pearson.

Ikebudu, O., chukwumuanya E. O, N. Swift O., and Toochukwu N. 2015. "Design of Pelletizing Machine(Balling Disc)." *International Journal of Materials, Mechanics and Manufacturing* 3.

Jawahar, N., and H. A. Patel. 2012. "Multi-Unit Particulates System (MUPS): "A Novel Pellets for Oral Dosage Forms." *Journal of Pharmaceutical Sciences and Research* 4(9):735673657.

Khurmi, R. S., and J. K. Gupta. 2008. *Theory of Machines*. 1st colour. India: Eurasia publishing House (P) Ltd.

Khurmi, R. S., and K. J. Gupta. 2008. *A Textbook on Machine Design*. 1st colour. India: Vikas publishing House Pvt Ltd.

Martin Sprocket & Gear, Inc. 2011. *Martin Catalogue - V Pulley*.

Milan, Dragan M., and Velimir. 2011. "Wood Pellets Production Technology" International Conference Safety of Technical Systems in Living and Working Environment." *Safety Engineering*.

de Moraes, Sandra Lúcia, José Renato Baptista de Lima, and Tiago Ramos Ribeiro. 2018. "Iron Ore Pelletizing Process: An Overview." Pp. 41–59 in *Iron Ores and Iron Oxide Materials,* edited by V. Shatokha. London: IntechOpen Limited, London.

Newitt, D. M., and J. M. Conway-Jones. 1958. "A Contribution to the Theory and Practice of Granulation." *Trans. Inst. Chem. Engrs.* 36(422).

Okechukwu, Ikebudu Kingsley. 2012. "Mechanized Balling Disc Machine (Pelletizer) for Industrial Development in Nigeria." *Lecture Notes in Engineering and Computer Science* 2:1427–32.

Omenyi, S. N., and C. E. Capes. 1982. "Correlation of Moist Strength with Contact Angles for Polymer Powder Agglomerates." *Powder Technology* 33:167–74.

Omenyi, S. N., A. E. Fouda, and C. E. Capes. 1983. "Some Surface Energy Effects in the Strength of Moist Polymer Agglomerates." *Chemical Engineering Science* 38(1):85–90. doi: 10.1016/0009-2509(83)80137-7.

Pathade, Phadtare D. G., and Saudagar R. B. 2014. "Pelletization. A Most Significant Technology in the Pharmaceuticals." *World Journal of Pharmaceutical Research* 3:1972–2003.

Rumpf, H. in (ed. .. W. A. Knepper. 1962. "Agglomeration." *Interscience, New York* 379.

Shardul, Vipul J., Arun M. Kulkarni, Amol S. Dayma, and Anvesh Virkunwar. 2018. "Design , Fabrication of Solar Operated Biomass Pelletizing Machine and Study of Biomass Pellet Samples." *International Research Journal of Engineering and Technology (IRJET)* 5(7):1524–35.

Sharma, P. C., and D. K. Aggarwal. 2013. *A Textbook of Machine Design*. Twelveth E. NEW DELHI: S. K. Kataria & Sons.

SKF. 2015. "SKF Stainless Stell Deep Groove Ball Bearings."

Szulc, Agnieszka, Ewa Skotnicka, Munish Kumar Gupta, and Jolanta Beata Królczyk. 2024. "Powder Agglomeration Processes of Bulk Materials – A State of the Art Review on Different Granulation Methods and Applications." *Powder Technology* 431:119092. doi: https://doi.org/10.1016/j.powtec.2023.119092.

Tondare, Anirudha, Anay Nadkar, Vishaka Zope, and Mohan P. Khond. 2018. "Design and Fabrication of Biomass Pelleting Machine." *Journal of Advancement in Machines* 3(3):6–11.

Udo, Mfon, David Esezobor, Adeniran Afolalu, Harrison Onovo, Samson Ongbali, and Imhade P. Okokpujie. 2018. "Investigation of Balling Characteristics of Mixture of Iron Oxide Bearing Wastes and Iron Ore Concentrates." Pp. 1–10 in *IOP Conference Series: Materials Science and Engineering*. Vol. 413.

Udo, Mfon O., D. E. Esezobor, F. I. Apeh, and Adeniran S. Afolalu. 2018. "Factors Affecting Ballability of Mixture Iron Ore Concentrates and Iron Oxide Bearing Wastes in Metallurgical Processing." *Journal of Ecological Engineering* 19(3):235–42. doi: 10.12911/22998993/86158.

Vo, T. T., P. Nezamabadi, S. Mutabaruka, J. Y. Delenne, R. J. M. Pellenq, E. Izard, and F. Radjai. 2018. "Micromechanics of the Granulation Process in Wet Granular Flows." in *In Engineering Mechanics Institute (EMI) Conference*.